The Astrophysical Journal, 600:451–457, 2004 January 1

SOLAR ENERGETIC PARTICLE ACCELERATION IN REFRACTING CORONAL SHOCK WAVES

Rami Vainio
Department of Physical Sciences, University of Helsinki, FIN-00014 Helsinki, Finland

and

Josef I. Khan[1,2]
Tuorla Observatory, University of Turku, FIN-21500 Piikkiö, Finland
Received 2003 May 2; accepted 2003 September 12

ABSTRACT

Gradual solar energetic particle (SEP) events are known to be correlated with coronal mass ejections (CMEs) and soft X-ray flares. The current paradigm of particle acceleration in these events attributes it to CME-driven shock waves in the solar corona and in interplanetary space. Even in small gradual SEP events related to CMEs with speeds in the (possibly submagnetosonic) range of 300–800 km s^{-1}, shock waves at global coronal scales, as evidenced by associated metric type II radio bursts, are important. Recent observational evidence from soft X-ray imaging data supports models of coronal shock wave propagation in the solar atmosphere as freely propagating blast waves that refract toward the solar surface as they propagate away from the flare site. Based on these observations, we study a model of test-particle acceleration in such a global refracting coronal shock wave. Such shocks may also be generated by solar eruptions other than flares, e.g., slow CMEs. The geometry of the shock wave results in the observer in the interplanetary medium being magnetically connected with the *downstream region* of the shock wave. Thus, steady-state diffusive shock acceleration predicts that the energy spectrum of the escaping ions is a power law, as typically observed—a result that is *not* obtained naturally if the observer is connected to the upstream region of the shock wave. Using parameters of upstream turbulence obtained from models of a cyclotron-heated solar corona, we calculate typical timescales of diffusive proton acceleration and show them to be consistent with the maximum proton energies typically observed in small, gradual SEP events. Acceleration in refracting coronal shock waves may also provide a preacceleration mechanism for further acceleration in CME-driven shocks in large gradual SEP events.

Subject headings: shock waves — Sun: corona — Sun: flares — Sun: particle emission

1. MOTIVATION

Solar energetic particle (SEP) events can be divided into two classes, i.e., impulsive and gradual events (e.g., Reames 1999). The former are usually relatively low-intensity and short-duration (from hours to days) events; they have ion abundances with strong enhancements of ^{3}He and heavy ions relative to coronal abundances and ion charge states exceeding typical coronal values. Typical maximum particle energies in these impulsive events are $\lesssim$10 MeV per nucleon, and the events are usually observable only if the accompanying flare occurs close to the nominal root (at $\sim$W60°) of the interplanetary (IP) magnetic field lines connected to the observer. The particles in these events are generally believed to be accelerated in impulsive solar flares (e.g., Reames 1999). In contrast, gradual SEP events have higher particle intensities and power-law energy spectra extending to higher energies (in the case of protons beyond 1 GeV in extreme cases), long durations (days to weeks), and typical coronal ion abundances and charge states (Reames 1999). They are well correlated with coronal mass ejections (CMEs) and gradual soft X-ray flares (Kahler, Hildner, & van Hollebeke 1978; Kahler et al. 1984), as well as with type II radio bursts (Švestka & Fritzová-Švestková 1974). Fast (>750 km s^{-1}) CMEs are likely to be super-magnetosonic and drive shock waves. Consequently, the most widely accepted mechanism for particle acceleration in gradual SEP events is diffusive shock acceleration in CME-driven shock waves in the solar corona and in IP space (see, e.g., Reames 1999 and references therein).

However, there is observational evidence that suggests that acceleration in CME-related SEP events might be more complicated than the simple bow shock picture suggests, especially if the CME speed is not very high. Kocharov et al. (2001) studied CMEs with speeds in the range 300–800 km s^{-1} observed by the Large Angle Spectroscopic Coronagraph (LASCO) (Brueckner et al. 1995) on board the *Solar and Heliospheric Observatory* (*SOHO*) (Domingo, Fleck, & Poland 1995). They found that all of those CMEs that were associated with SEP events observed by the Energetic and Relativistic Nuclei and Electron Experiment (ERNE) (Torsti et al. 1995) on board *SOHO*, rapidly (within 2–4 $R_\odot$) accelerated to a constant speed measured within the coronagraph field of view. In addition, 95% of the SEP-related CMEs were related to soft X-ray flares and 63% to metric type II radio bursts. For all rapidly accelerating CMEs in this speed range, i.e., not only those that were SEP-related, these percentages were significantly lower: 67% were associated with soft X-ray flares and only 15% with metric type II burst. The authors concluded that "a typical SEP-producing CME [with a speed in the range 300–800 km s^{-1}] experiences fast acceleration close to the Sun associated with soft X-ray flare and coronal shocks." This conclusion is backed up by a number of detailed case studies (e.g., Torsti et al. 1998, 1999a, 1999b, 2001) suggesting that shock waves

[1] Current address: Department of Physics and Astronomy, University of Glasgow, Glasgow G12 8QQ, UK.
[2] The Tuorla Observatory is part of the Väisälä Institute for Space Physics and Astronomy, University of Turku.

on global coronal size scales (of about 1 $R_\odot$) are necessary for particle acceleration associated with moderate speed CMEs.

Type II radio bursts observed in radio spectrograms at metric wavelengths provided the first indirect evidence of shock waves propagating in the solar corona (Wild, Smerd, & Weiss 1963; Uchida 1960; Wild & Smerd 1972), long before the CME era. Since then, type II radio bursts have been observed from decimetric to kilometric wavelengths. Type II bursts are believed to originate from the conversion of electrostatic plasma emission produced at a weak fast-mode MHD shock front (Uchida 1960; Mann 1995). A distinction is generally made between type II radio bursts observed at decimetric metric wavelengths, referred to as coronal type II bursts, and hectometric kilometric wavelengths, referred to as IP type II radio bursts. While IP type II bursts are usually ascribed to bow shock waves driven ahead of a CME piston (Kahler 1992), the proposed origins for coronal type II bursts are still debated. Some suggest that these are CME driven, like IP shocks (Cliver, Webb, & Howard 1999). However, coronal type II bursts are known to have a close temporal association with solar flares (Swarup, Stone, & Maxwell 1960; Dodge 1975; Cane & Reames 1988). It has been suggested that they may be due to shock waves driven by flare-associated mass motions such as flare ejecta (Gopalswamy et al. 1997, 1998) or chromospheric evaporation flows (Karlický & Odstrčil 1994). Alternatively, it has been suggested that they are due to freely propagating blast waves caused by flare explosions (Uchida 1974).

Wavelike disturbances have sometimes been observed in the chromosphere propagating away from flaring regions. These waves, observed in Hα and off-band Hα and referred to as Moreton waves (Moreton 1960), were interpreted by Uchida (1968) as the flanks of large-scale coronal blast waves. Since the launch of *SOHO*, similar disturbances have been observed to propagate through the corona. Specifically, the Extreme Ultraviolet Imaging Telescope (EIT) (Delaboudiniére et al. 1995) detected Moreton-wave–like or shock-wave–like disturbances, so-called EIT waves, at coronal heights associated with flares and/or CMEs (e.g., Thompson et al. 1999). Similar waves have recently been reported in the He I 1083 nm line by Vršnak et al. (2002). These have been interpreted as due to coronal shock waves giving rise to emission in the transition region. Both Moreton waves (Cliver et al. 1995) and EIT waves (Torsti et al. 1998, 1999a) have also been associated with rapid SEP access to Earth-connected magnetic field lines in SEP events associated with angle-distant flares.

Recently, coronal shock waves have been observed in soft X-ray images (Khan & Aurass 2002). Soft X-ray images provide direct observations of coronal shock waves and thus of their morphology and physical properties in the corona. Hudson et al. (2003) reported soft X-ray observations of a shock wave observed with high temporal and spatial resolution. Among their findings was clear observational evidence for the bending (refraction) of the coronal wave toward the solar surface as it moved away from the flare—as predicted in the blast wave model of Uchida (1968, 1970, 1974) and Uchida, Altschuler, & Newkirk (1973). This bending occurs because the Alfvén speed in the solar corona increases with height at distances close to the Sun below about 2 $R_\odot$.

In addition to flare explosions, other types of coronal energy releases may lead to refracting shock waves as well; e.g., mass motions associated with the liftoff of a slow CME in the corona may act as a source of large-amplitude magnetosonic waves, which escape the expanding (but still rather localized) disturbance. Such waves would quickly steepen to shock waves that would propagate freely in the corona at large distances from the site of initial energy release. Given the fact that (presumably confined) impulsive flares produce SEP events that are different (e.g., in composition) from the gradual ones and thus not attributed to shocks, we suggest that some kind of an eruptive process is necessary to generate shock waves capable of particle acceleration in the solar corona.

In this paper, we study particle acceleration in such refracting coronal shock waves. We begin by reviewing the key results of diffusive shock acceleration theory and introducing the available observational constraints in § 2. We then proceed to present a model of particle acceleration in refracting shocks and evaluate its key parameters in § 3. Finally, a discussion along with conclusions are presented in § 4.

2. DIFFUSIVE SHOCK ACCELERATION IN SOLAR CORONA

Diffusive shock acceleration (e.g., Bell 1978) is probably the most widely employed mechanism of particle acceleration for the numerous energetic particle populations filling the universe. In this mechanism, a particle gains energy from the bulk plasma flow by scattering off magnetic irregularities that are converging on the shock. The mechanism is efficient and simple and naturally produces a power-law energy spectrum (with a high-energy cutoff) that is the most common spectral form deduced to be emitted from the source in the case of SEPs (e.g., Ellison & Ramaty 1985). The differential particle intensity, dJ/dE, at the shock (and below the cutoff energy) is determined by the *scattering center compression ratio* $\rho_{\rm sc} = u_{1n}/u_{2n}$,

$$\frac{dJ_S}{dE} = p^2 f(p) \propto p^{-\sigma}; \quad \sigma = \frac{\rho_{\rm sc} + 2}{\rho_{\rm sc} - 1}, \tag{1}$$

where $u_{1n[2n]}$ is the speed of the scattering centers (i.e., the magnetic irregularities) relative to the shock in the ambient [shocked] plasma, measured along the shock normal, and p is the particle momentum. This power law extends from the suprathermal injection energies up to the cutoff energy determined, e.g., by the available acceleration time or geometric effects (Vainio 1999). Hereafter, we follow the usual convention and consider the frame of reference moving with the shock wave. Consequently, the region of shocked plasma (behind the shock front) is referred to as the downstream region, while the region of undisturbed plasma (ahead of the shock) is referred to as the upstream region.

There are some key observational constraints that a theory of SEP acceleration has to explain. From the time lags of the SEPs relative to the electromagnetic emission (e.g., flare), we can deduce that typical timescales for the protons to attain energies above 10 MeV should not exceed some tens of minutes. These are also typical timescales for coronal shocks to expand over global coronal scales of about 1 $R_\odot$ (Torsti et al. 1998, 1999a, 1999b, 2001). The timescale of momentum gain by diffusive shock acceleration, τ_p, depends on the particle scattering mean free path λ (which determines the typical time between successive shock crossings). If scattering in the downstream region is very rapid, the result is (e.g., Drury 1983; Vainio 1999)

$$\tau_p = \frac{p}{\dot{p}} \approx \frac{3\rho_{\rm sc}}{\rho_{\rm sc} - 1} \frac{\kappa_n}{u_{1n}^2} = \frac{\rho_{\rm sc}}{\rho_{\rm sc} - 1} \frac{v\lambda}{u_{1n}^2} \left(\cos^2\theta_n + \mathcal{R}_\perp \sin^2\theta_n\right), \tag{2}$$

where $\kappa_n = \frac{1}{3} v\lambda \left(\cos^2\theta_n + \mathcal{R}_\perp \sin^2\theta_n\right)$ is the spatial diffusion coefficient normal to the shock front, θ_n is the angle between

the shock normal and the upstream magnetic field, v is the particle speed, and $\mathcal{R}_\perp = \kappa_\perp/\kappa_\parallel \ll 1$ is the ratio of the diffusion coefficients perpendicular ($\kappa_\perp$) and parallel ($\kappa_\parallel = \frac{1}{3}\lambda v$) to the mean magnetic field. Note that diffusion perpendicular to the mean field is primarily due to the random walk of the field lines themselves. We adopt $\mathcal{R}_\perp = 0$, which is a good approximation in the solar corona (where fluctuations are weak compared to the mean field, $\delta B \ll B$) unless the shock normal is almost perpendicular to the ambient magnetic field ($\theta_n \approx 90^\circ$). Adopting a mean free path proportional to particle momentum—i.e., $\lambda = \lambda_0(p/p_0)$, where $\lambda_0 = \lambda(p_0)$ and p_0 is an arbitrary scaling momentum—allows us to estimate the maximum energies attainable by diffusive shock acceleration. We integrate the equation for momentum gain over time from the time of particle injection at low energies, $t = t_0$, to time $t = t_0 + \Delta t$ to get the change in energy

$$\Delta E = \int_{t_0}^{t_0+\Delta t} v\, dp \approx \frac{\rho_{\rm sc} - 1}{\rho_{\rm sc}} \frac{p_0 u_{1n}^2}{\cos^2\theta_n \lambda_0} \Delta t, \tag{3}$$

assuming all the parameters to be constant in time. Taking $\Delta t \lesssim R_S\ R_\odot/u_{1n}$ and $u_{1n} = u_{-3} \times 10^{-3} c$, where R_S and u_{-3} are constants of the order unity and c is the speed of light, we get

$$\Delta E \lesssim p_0 c \frac{\rho_{\rm sc} - 1}{\rho_{\rm sc}} u_{-3} R_S \frac{10^{-3}\ R_\odot}{\cos^2\theta_n \lambda_0}. \tag{4}$$

If we take $p_0 c = 140$ MeV (corresponding to $E_0 = 10$ MeV proton energy), we get

$$\Delta E \lesssim E_0 \frac{\rho_{\rm sc} - 1}{\rho_{\rm sc}} u_{-3} R_S \frac{1.4 \times 10^{-2}\ R_\odot}{\cos^2\theta_n \lambda_0}. \tag{5}$$

Thus, to accelerate protons to energies $E > E_0 = 10$ MeV starting from much lower energies, the shock has to propagate into a medium with a very short scattering mean free path, less than 1 $R_\odot$ at 10 MeV, if $\theta_n \lesssim 80^\circ$. This favors particle acceleration close to the Sun (where the shocks can be almost perpendicular) rather than in the outer corona (where we expect shocks to propagate predominantly parallel to the ambient magnetic field).

As demonstrated above, to effectively accelerate particles, such shock waves need to propagate into a very turbulent medium. The ambient turbulence, however, needs to be specially arranged in front of such shocks to explain (simultaneously with the efficient acceleration) the observed fast propagation of particles in the IP medium. For ambient coronal turbulence, one needs to restrict the turbulent region somehow (e.g., via damping connected with coronal heating) to distances close to the Sun, i.e., well below $\sim 10\ R_\odot$ (Vainio & Laitinen 2001), to allow the particles to escape quickly enough from the acceleration region.

Even if one succeeds in explaining the efficient scattering near the shock simultaneously with the fast transport away from it, there is another issue that needs to be addressed. As noted by Vainio, Kocharov, & Laitinen (2000), the energy spectrum of the accelerated particles escaping to the ambient medium is given by

$$\frac{dN_1}{dE} \propto \frac{1}{v(e^{\eta_1} - 1)} \frac{dJ_S}{dE} \propto e^{-\eta_1(E)} E^{-(\sigma+1)/2}, \tag{6}$$

where $dJ_{S/dE}$ is the differential intensity at the shock. Here we have restricted consideration to nonrelativistic energies. Here, $\eta_1(E) = L_1/L_D$ is the (large) number of diffusion lengths, $L_D = \kappa_n/u_{1n}$, in the turbulent upstream region between the shock and the free escape boundary located at distance L_1 ahead of the shock. (This is the distance at which turbulence is so weak that it can no longer trap the particles.) The energy spectrum of particles escaping far downstream is

$$\frac{dN_2}{dE} \propto \frac{1}{v} \frac{dJ_S}{dE} \propto E^{-(\sigma+1)/2}. \tag{7}$$

Thus, diffusive shock acceleration predicts a power-law spectrum to be observed far *downstream* of the acceleration region. However, the spectrum emitted from the shock toward the ambient medium can be significantly suppressed at low energies, since $\eta_1(E)$ decreases with energy if L_1 is independent of energy and $\kappa_n(E)$ increases with it. This may not be consistent with SEP observations that show power-law emission from the Sun early in the event (e.g., Torsti et al. 1999b). The prediction of hard, curved upstream spectra is quite common in test-particle acceleration theories and can be overcome only by considering an energy-independent diffusion coefficient (see, e.g., Lee & Ryan 1986 for such a model). Note, however, that the requirement of constant or logarithmically energy-dependent η_1 (to ensure a power-law energy spectrum of particles escaping toward the ambient medium) may be automatically satisfied in shock acceleration models employing self-generated turbulence, as discussed in § 4.

CME shock acceleration in the solar corona at intermediate distances, ~ 2–$4\ R_\odot$, may have a further inhibiting factor: the maximum value of the coronal Alfvén speed, $V_{\rm A}$, outside active regions and coronal holes is located at these distances, and can be high, from about 600 km s^{-1} to about 1000 km s^{-1} depending on the model of density and magnetic field used to evaluate $V_{\rm A}$. Within both active regions and coronal holes, typical Alfvén speeds are a few thousand km s^{-1}. Examples of modeled coronal Alfvén speeds with heliocentric distance are shown in Figure 1. We have used a magnetic field of $B = 1.7\ (R_\odot/R)^3 + 1.3\ (R_\odot/R)^2$ G, which is appropriate for equatorial regions. This model is combined with three electron density models, those of Saito, Poland, & Munro (1977), Sittler &

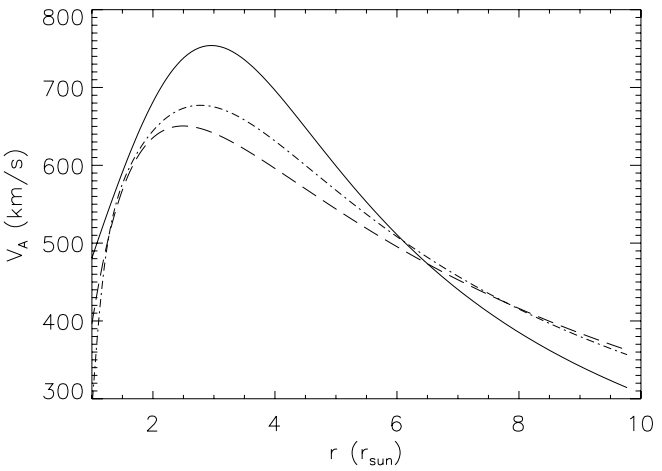

FIG. 1.—Coronal Alfvén speed as a function of heliocentric distance. The three curves are calculated using a magnetic field of $B = 1.7\ (R_\odot/R)^3 + 1.3\ (R_\odot/R)^2$ G and the density models of Saito et al. (1977) (*solid curve*), Sittler & Guhathakurta (1999) (*dashed curve*), and Newkirk (1967) (*dot-dashed curve*).

Guhathakurta (1999), and Newkirk (1967), for the equatorial background corona assuming a 5% He content in the plasma to calculate the mass density. The maximum values of V_A are located between 2.5 and 3.0 $R_\odot$, and the maximum values are between 650 and 750 km s^{-1}. The region where the Alfvén speed exceeds 600 km s^{-1} extends from $\sim$1.6 to 4.5 $R_\odot$. Thus, CMEs with speeds in the range of less than 600 km s^{-1} may not be able to drive shocks at these distances. The Alfvén speed is lower closer to the solar surface, a few hundred km s^{-1}, again for typical (equatorial) coronal densities and magnetic fields outside active regions, favoring the quiet equatorial low corona as a site for shock acceleration.

We next consider a simplified model of coronal shock acceleration, in which the shock wave has a reverse-type geometry in the vicinity of the solar surface caused by its bending toward the photosphere. We model the scattering of energetic protons between the shock and the solar surface by assuming it to be due to high-frequency Alfvén waves emitted from the surface with the energy flux needed to explain the heating of the corona. With this information, we estimate the maximum proton energies obtained from our model and compare them with typically observed spectral cutoffs in small gradual events.

3. SOLAR ENERGETIC PARTICLE ACCELERATION IN A REFRACTING SHOCK WAVE

We consider a freely propagating shock wave moving in the solar corona. The shock near the solar surface is connected to a larger global wave structure (see Fig. 2). However, the regions of the wave at large heights ($R \gtrsim 2\ R_\odot$) from the solar surface are assumed to be weak in particle acceleration because of the high Alfvén speeds, quasi-parallel shock geometries, and much lower levels of ambient turbulence (to allow fast SEP escape) at these heights. A key element in our model is that the observer in IP space is magnetically connected to the *downstream region* of the shock wave. We follow Vršnak et al. (2002) and assume that the associated metric type II radio burst is generated in the vicinity where the shock wave has a perpendicular geometry, since this presumably offers the most favorable conditions for electron acceleration. A (chromospheric) Moreton wave front is assumed to be the sweeping skirt of the coronal shock in the chromosphere. Note that an associated slow (sub-Alfvénic) CME may be embedded within the global magnetic structure without making the model invalid.

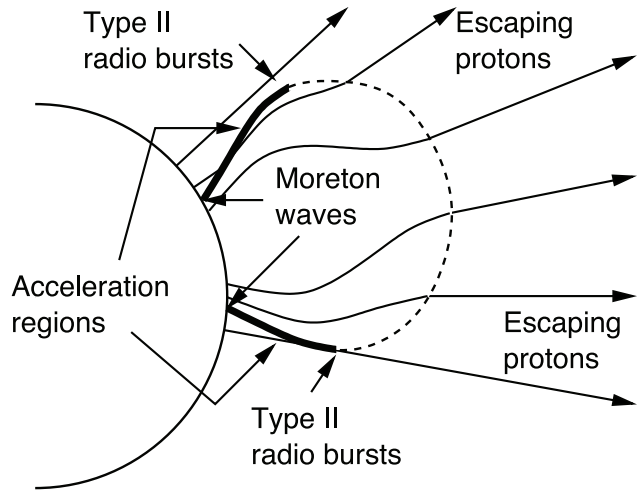

FIG. 2.—Global shock geometry in our model. The expanding shock is strong where the Alfvén speed is low, i.e., in the overturning regions close to the Sun. Thus, protons observed in the interplanetary medium are the ones escaping to the far *downstream region* of the shock.

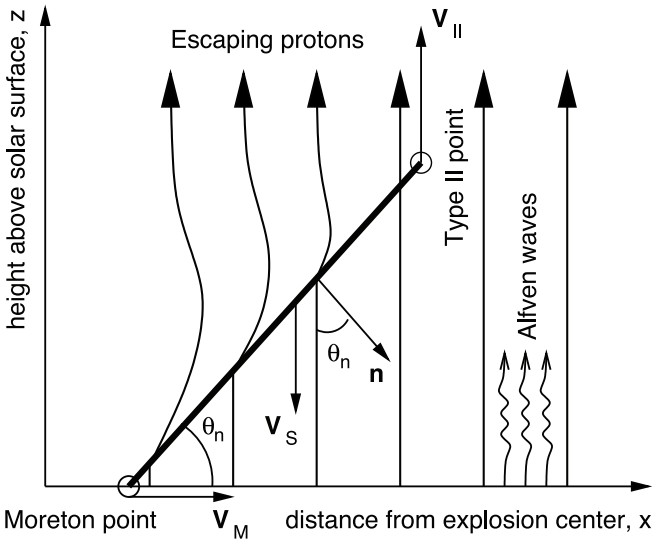

FIG. 3.—Simplified model of the acceleration region. V_M is the Moreton wave speed, θ_n is the (constant) angle between the shock normal $\boldsymbol{n}$ and the magnetic field, V_{II} is the vertical speed deduced from the metric type II drift rate, and $V_S = V_M \tan\theta_n$ is the shock speed projected along the field lines.

Let us consider proton acceleration in a simplified reverse-type coronal shock wave geometry (i.e., with a projected component of velocity, $\boldsymbol{V}_S$, along the magnetic field, which points *toward* the Sun), as depicted in Figure 3. For simplicity, let us assume that the shock wave propagates maintaining a fixed normal angle θ_n relative to the upstream (vertical) field lines and that its velocity component parallel to the solar surface is given by the Moreton wave speed, V_M, that may be observed. Thus, in the (de Hoffmann–Teller) shock frame, the upstream flow speed along the field lines is $V_S = V_M \tan\theta_n$ toward the shock. A lower limit of this speed is provided by the requirement that the shock must be super-Alfvénic, $V_S \cos\theta_n \equiv MV_A > V_A$, i.e., $V_M = MV_A/\sin\theta_n > V_A/\sin\theta_n$, where $M = V_S \cos\theta_n/V_A$ is the (Alfvénic) Mach number of the shock.

As noted above, the steady-state energy spectrum of accelerated particles emitted downstream of the shock wave is a power law given by equation (7). This power law continues up to a cutoff energy, E_c, determined by the shock geometry and/or lifetime, after which the spectrum softens with an exponential-type rollover. The exact functional form of the spectrum at $E \gtrsim E_c$ depends on the cutoff mechanism; see Vainio (1999) for examples. In our simplified plane geometry, the cutoff momentum is determined by the available acceleration time, $T_S = z_0/V_S$, where z_0 is the height above the solar surface of the point where the shock (i.e., the point of type II emission) first intersects the observer's magnetic field line at time t_0.

Let us first use observations of SEP energy spectra to estimate typical scattering center compression ratios needed to explain the data. SEP transport in the IP medium can often be approximated as radial diffusion. For a constant radial mean free path of $\lambda_{rr} \sim 0.1$ AU and an impulsive injection at the Sun, this implies that the differential particle intensities near the Earth peak at $t = t_{\max}(E) \approx \tau_{IP}(E) \equiv R_\oplus^2/(2\lambda_{rr}v)$, where $R_\oplus = 1$ AU, giving $\tau_{IP} \sim 5$ hr at $E \sim 10$ MeV. In our model,

the injection of particles is short compared to $\tau_{\rm IP}$. Thus, the measured differential particle intensity, $I(E,t) \equiv |dJ/dE|_{R=R_\oplus}$, can be related to the energy spectrum emitted from the source, dN_2/dE, as

$$I(E, t_{\max}) \propto v \frac{dN_2}{dE} \propto E^{-\sigma/2}. \quad (8)$$

This approximation neglects the effects of adiabatic deceleration during IP transport, which would act to harden the observed spectrum at low energies. Typically observed spectral indices are $\sigma/2 \sim 1$–3 (e.g., Torsti et al. 2001), giving an estimate of the typical scattering center compression ratio as $\rho_{\rm sc} \sim 1.6$–4. Note that especially for low Mach number shocks, the scattering center compression ratio is not identical to the gas compression ratio, ρ_g. At least in parallel shock waves, the former can be relatively large even in shocks with ρ_g close to 1 (Vainio & Schlickeiser 1999).

To calculate the maximum energy in the emitted spectrum of particles, we still need to estimate u_{1n} and λ. Following Vainio & Laitinen (2001), we assume the upstream scattering occurs off of high-frequency Alfvén waves emitted from the Sun. Thus, the scattering center speed (along the field lines) in the shock frame is not the fluid speed but is given by $u_1 = V_S + V_{\rm A}$ (Vainio & Schlickeiser 1998, 1999), resulting in $u_{1n} = u_1 \cos\theta_n = (V_S + V_{\rm A})\cos\theta = V_{\rm A}(M + \cos\theta_n)$.

To be able to calculate λ, we need an estimate for the mean free path determined by the Alfvén wave power spectrum in the solar corona. This can be obtained from the models of coronal heating that employ cyclotron damping of high-frequency Alfvén waves (e.g., Tu & Marsch 1997; Laitinen, Fichtner, & Vainio 2003). High and anisotropic ion temperatures and large nonthermal velocities observed in coronal holes (Kohl et al. 1998) support this model of coronal heating on open field lines. Using an Alfvén wave spectrum typically employed in wave-heating models, Vainio & Laitinen (2001) obtained mean free paths near the solar surface of $\lambda \approx \lambda_0 (p/p_0) V_{\rm A}(R)/V_{\rm A}(R_\odot)$ with $\lambda_0 = 0.04\ R_\odot$ and $p_0 = mc$, where m is the particle mass. In the model of the coronal magnetic field and density used by Vainio & Laitinen (2001), the Alfvén speed is $V_{\rm A}(R_\odot) = 200$ km s^{-1} at the solar surface but increases rather rapidly to above 1000 km s^{-1}. Taking $V_{\rm A} = 500$ km s^{-1} as a representative value in the acceleration region, we get $\lambda = \lambda_0 (p/p_0)$ with $\lambda_0 = 0.1\ R_\odot$ and $p_0 = mc$.

Next, we substitute the values of $\rho_{\rm sc} = 2$ (corresponding to $\sigma/2 = 2$), $\lambda_0 = 0.1\ R_\odot$, $u_{1n} = V_{\rm A}(M + \cos\theta_n)$, $V_{\rm A} = 500$ km s^{-1}, $p_0 = mc$, and $\Delta t = T_S = z_0 \cos\theta_n / M V_{\rm A}$ in equation (3) to obtain an estimate for the spectral cutoff energy

$$E_c \sim \frac{\rho_{\rm sc} - 1}{\rho_{\rm sc}} \frac{mcV_{\rm A}^2 (M + \cos\theta_n)^2}{\lambda_0 \cos^2\theta_n} \frac{z_0 \cos\theta_n}{MV_{\rm A}}$$
$$= E_{c0} \frac{(M + \cos\theta_n)^2}{4M\cos\theta_n} \frac{z_0}{R_\odot} > E_{c0} \frac{z_0}{R_\odot}, \quad (9)$$

where $E_{c0} = 40 mcV_{\rm A}(\rho_{\rm sc} - 1)/\rho_{\rm sc} \approx 30$ MeV for our chosen parameters. Note that because of our assumption of $\mathcal{R}_\perp = 0$, we have to restrict consideration to angles where $\cos^2\theta_n \gg \mathcal{R}_\perp$. Thus, very small values of the denominator are not possible, and values of a few tens of MeV are expected as an outcome of our model.

Finally, we try eliminate some of the remaining parameters using typically observed values for the component of the type II speed, $V_{\rm II}$, as seen in a radio spectrogram, and $V_{\rm M}$. We note that the sideways expansion speed of the Type II point has to be $\dot{x}_{\rm II} \approx V_{\rm M} + V_{\rm II}\tan\theta_n$ (see Fig. 3) so that the time $t_0 \approx x/(V_{\rm M} + V_{\rm II}\tan\theta_n)$. Here x is the horizontal distance from the center of the explosion to the observer's field line, which can be estimated if the flare site is known. At time t_0, the type II point is therefore at a height of $z_0 = V_{\rm II} t_0 \approx x V_{\rm II}/(V_{\rm M} + V_{\rm II}\tan\theta_n)$, assuming an explosion at the solar surface. Thus, one of the parameters, z_0 or θ_n, could be eliminated in favor of the other. The estimate also shows that $z_0 < x V_{\rm II}/V_{\rm M}$, providing an upper limit for this parameter. Note, however, that an Alfvén speed varying as a function of height results in a nonconstant θ_n during the shock wave propagation, which makes these estimates rather uncertain.

4. DISCUSSION AND CONCLUSIONS

We have modeled energetic proton acceleration in coronal shock waves propagating close to the solar surface on open coronal field lines. Such shocks have a reverse-type geometry; i.e., the observer in IP space is magnetically connected to the *downstream* region of the shock wave. The model is capable of explaining the observed power-law energy spectra in small gradual SEP events. We noted that power-law spectra are not easily produced by the diffusive shock acceleration mechanism if the observer is connected to the upstream region of the shock wave. In such a case one would instead expect a preferred escape of high-energy particles from the shock, because the escape is controlled by the turbulent trapping ahead of the shock, which is substantially more efficient for low-energy particles than for high-energy particles, at least in test-particle models, in which the particle mean free path would be an increasing function of energy and the size of the upstream trapping region independent of energy. In contrast, our model, where the escape of particles is due to downstream convection away from the shock, yields a power-law energy spectrum for the escaping particles, as long as a power-law spectrum is produced at the shock. By considering plausible timescales of particle acceleration in our model shock waves, we deduced that the power-law energy spectrum should extend up to a few tens of MeV, after which there should be spectral softening. Values of $E_c \gtrsim 10$ MeV are typically observed in small gradual events (e.g., Anttila & Sahla 2000), and since many of these events are accompanied by metric type II bursts (Kocharov et al. 2001) and EIT waves (Torsti et al. 1998, 1999a), our model provides a simple and natural way to explain SEP acceleration in these events.

The special conditions required for the upstream turbulence for forward-type shock waves can alternatively be provided by relating the turbulence to the shock itself. A model with a narrow ($<1\ R_\odot$) turbulent region comoving with the shock and followed by a region of scatter-free transport farther outward was analyzed by Vainio et al. (2000) and found to be capable of producing observed particle spectra in a reasonable acceleration time. In the large gradual events, streaming instabilities of the accelerated protons themselves (Bell 1978) may produce turbulence that is very intense near the shock but rapidly weakens farther away from the shock in the upstream region. If the background wave intensities are small, this mechanism predicts a hard power-law spectrum (with $\sigma = 1$) far upstream, thus better fulfilling the constraints set by observed SEP spectra (Bell 1978; Reames 1999; Vainio 2003). In a sense, this mechanism automatically produces an upstream trapping region of a size suitable for generating a power-law spectrum of escaping particles. The same mechanism (Lee 1983) can

successfully explain (Kennel et al. 1986) energetic storm particle events connected with traveling IP shocks, observed below a few MeV. The model of self-generated waves has been used, for example, to explain the so-called streaming-limited proton intensities (Ng & Reames 1994; Reames & Ng 1998; Vainio 2003) and the time evolution of ion abundances during large gradual SEP events (Ng, Reames, & Tylka 1999). It is therefore plausible that this mechanism can explain (most of) the SEP acceleration in the largest events, usually related to the fastest CMEs (Kahler et al. 1984), but it is unlikely that enough waves could be generated to explain acceleration in events related to slower CMEs, which have typical proton intensities that fall 2–3 orders of magnitude below the streaming-limited intensities at 1 AU. Recently, Vainio (2003) showed that amplification of coronal Alfvén waves above background intensities requires a relatively large number of protons injected into a flux tube, i.e., a few times $10^{32}/E$ protons per steradian at the solar surface. In proton events with 1 MeV proton peak intensities below ~ 10 (cm^2 sr s MeV)$^{-1}$ at 1 AU, the coronal proton injection spectrum was considered unlikely to exceed the threshold for efficient wave amplification, and models other than the standard bow shock acceleration need to be developed for these events. Thus, our test-particle modeling seems appropriate for that purpose.

The reverse shocks would, of course, still be capable of particle acceleration even in the large events, but the escaping proton fluxes would probably be injected into the CME-driven shock from behind, because that driven shock could also intersect the field line connected to the observer (cf. Fig. 2, and consider, e.g., a CME inside the outer parts of the wave structure). Then the SEPs would be reaccelerated and/or trapped by the CME-driven shock. Thus, in larger events, coronal shock acceleration, as described in this paper, may provide a preacceleration mechanism for the IP shock, helping it to accelerate particles up to the highest energies.

If the CME starts driving a shock wave only in the outer corona, e.g., as proposed by Gopalswamy et al. (1998), acceleration in refracting coronal shocks could explain the double-peaked intensity time profiles observed in some gradual SEP events (e.g., Torsti et al. 1996; Laitinen et al. 2000), where a promptly (at heights below 1 $R_\odot$ from the surface) accelerated component is followed by a delayed main injection component. The prompt particle emission component could be attributed to acceleration by the reverse shock at early times of the eruption, whereas the (more intensive) delayed component is accelerated by the CME bow shock at larger distances of $\gtrsim 5$ $R_\odot$ from the Sun (Kahler 1994). The delayed component would be a mixture of freshly injected particles and reaccelerated prompt component particles. Note, however, that if the prompt component produces large proton intensities at 1 AU, streaming instabilities would also have to be taken into account in the modeling of the reverse shock acceleration. Because the upstream waves in our model are the stable ones, i.e., propagating from the photosphere toward the shock, streaming protons act to reduce the upstream turbulence level (and/or the scattering center compression ratio, if unstable waves are generated), so their effect may, in fact, be to *reduce* the maximum energy attained by the protons (and/or *increase* the spectral index). In any case, a calculation employing self-generated waves in the reverse shock configuration would be an interesting subject for future research.

In conclusion, we find that refracting coronal shock waves (1) can emit power-law energy spectra of accelerated protons extending up to tens of MeVs toward the IP medium, thus explaining observations in small gradual SEP events; (2) may provide a preacceleration mechanism for further acceleration in IP shocks driven by fast CMEs; and (3) may, together with the IP shocks, explain the double-peaked intensity profiles observed in some SEP events.

J. I. K. acknowledges financial support from the Academy of Finland. We are grateful to the referee for useful comments on the manuscript.

REFERENCES

Anttila, A., & Sahla, T. 2000, Ann. Geophys., 18, 1373
Bell, A. R. 1978, MNRAS, 182, 147
Brueckner, G. E., et al. 1995, Sol. Phys., 162, 357
Cane, H. V., & Reames, D. V. 1988, ApJ, 325, 895
Cliver, E. W., Webb, D. F., & Howard, R. A. 1999, Sol. Phys., 187, 89
Cliver, E. W., et al. 1995, Proc. 24th Int. Cosmic-Ray Conf. (Rome), 257
Delaboudiniére, J.-P., et al. 1995, Sol. Phys., 162, 291
Dodge, J. C. 1975, Sol. Phys., 42, 445
Domingo, V., Fleck, B., & Poland, A. I. 1995, Sol. Phys., 162, 1
Drury, L. O'C. 1983, Rep. Prog. Phys., 46, 973
Ellison, D. C., & Ramaty, R. 1985, ApJ, 298, 400
Gopalswamy, N., Kundu, M. R., Manoharan, P. K., Raoult, A., Nitta, N., & Zarka, P. 1997, ApJ, 486, 1036
Gopalswamy, N., et al. 1998, J. Geophys. Res., 103, 307
Hudson, H. S., Khan, J. I., Lemen, J. R., Nitta, N. V., & Uchida, Y. 2003, Sol. Phys., 212, 121
Kahler, S. 1992, ARA&A, 30, 113
———. 1994, ApJ, 428, 837
Kahler, S. W., Hildner, E., & van Hollebeke, M. A. I. 1978, Sol. Phys., 57, 429
Kahler, S. W., et al. 1984, J. Geophys. Res., 89, 9683
Karlický, M., & Odstrčil, D. 1994, Sol. Phys., 155, 171
Kennel, C. F., et al. 1986, J. Geophys. Res., 91, 11917
Khan, J. I., & Aurass, H. 2002, A&A, 383, 1018
Kocharov, L., Torsti, J., St. Cyr, O. C., & Huhtanen, T. 2001, A&A, 370, 1064
Kohl, J. L., et al. 1998, ApJ, 501, L127
Laitinen, T., Fichtner, H., & Vainio, R. 2003, J. Geophys. Res., 108, 1081
Laitinen, T., et al. 2000, A&A, 360, 729
Lee, M. A. 1983, J. Geophys. Res., 88, 6109
Lee, M. A., & Ryan, J. M. 1986, ApJ, 303, 829
Mann, G. 1995, in Coronal Magnetic Energy Releases, ed. A. O. Benz & A. Krüger (Berlin: Springer), 183
Moreton, G. E. 1960, AJ, 70, 494
Newkirk, G., Jr. 1967, ARA&A, 5, 213
Ng, C. K., & Reames, D. V. 1994, ApJ, 424, 1032
Ng, C. K., Reames, D. V., & Tylka, A. J. 1999, Geophys. Res. Lett., 26, 2145
Reames, D. V. 1999, Space Sci. Rev., 90, 413
Reames, D. V., & Ng, C. K. 1998, ApJ, 504, 1002
Saito, K., Poland, A. I., & Munro, R. H. 1977, Sol. Phys., 55, 121
Sittler, E. C., Jr., & Guhathakurta, M. 1999, ApJ, 523, 812
Švestka, Z., & Fritzová-Švestková, L. 1974, Sol. Phys., 36, 417
Swarup, G., Stone, P. H., & Maxwell, A. 1960, ApJ, 131, 725
Thompson, B. J., et al. 1999, ApJ, 517, L151
Torsti, J., Kocharov, L., Innes, D. E., Laivola, J., & Sahla, T. 2001, A&A, 365, 198
Torsti, J., Kocharov, L., Teittinen, M., & Thompson, B. J. 1999a, ApJ, 510, 460
Torsti, J., Kocharov, L., Vainio, R., Anttila, A., & Kovaltsov, G. A. 1996, Sol. Phys., 166, 135
Torsti, J., et al. 1995, Sol. Phys., 162, 505
———. 1998, Geophys. Res. Lett., 25, 2525
———. 1999b, J. Geophys. Res., 104, 9903
Tu, C.-Y., & Marsch, E. 1997, Sol. Phys., 171, 363
Uchida, Y. 1960, PASJ, 12, 376
———. 1968, Sol. Phys., 4, 30
———. 1970, PASJ, 22, 341
———. 1974, Sol. Phys., 39, 431

Uchida, Y., Altschuler, M. D., & Newkirk, G., Jr. 1973, Sol. Phys., 28, 495
Vainio, R. 1999, in Plasma Turbulence and Energetic Particles in Astrophysics, ed. M. Ostrowski & R. Schlickeiser (Kraków: Obs. Astron., Uniw. Jagielloński), 232
———. 2003, A&A, 406, 735
Vainio, R., Kocharov, L., & Laitinen, T. 2000, ApJ, 528, 1015
Vainio, R., & Laitinen, T. 2001, A&A, 371, 738
Vainio, R., & Schlickeiser, R. 1998, A&A, 331, 793
———. 1999, A&A, 343, 303
Vršnak, B., Warmuth, A., Brajsa, R., & Hanslmeier, A. 2002, A&A, 394, 299
Wild, J. P., & Smerd, S. F. 1972, ARA&A, 10, 159
Wild, J. P., Smerd, S. F., & Weiss, A. A. 1963, ARA&A, 1, 291